Transformation-Induced Nonthermal Neutrino Spectra and Primordial Nucleosynthesis

Kevork Abazajian, Xiangdong Shi, and George M. Fuller

Department of Physics, University of California, San Diego, La Jolla, California 92093-0350

(September 17, 1999)

We examine in detail the changes in the production of primordial helium resulting from nonthermal neutrino momentum distributions produced by resonant transformation of electron-type neutrinos to steriles. These transformations, $\bar{\nu}_e \to \bar{\nu}_s$ ($\nu_e \to \nu_s$), amplify a positive (negative) lepton number asymmetry. We find that the resulting supression relative to a thermal distribution of low energy ν_e reduces $n \to p$ conversion to a greater extent than does the enhancement of $n \to p$ from an identical suppression of $\bar{\nu}_e$. Thus, equal lepton-number asymmetries of opposite sign have unequal effects on the resulting helium yield in primordial nucleosynthesis.

PACS numbers: 14.60.Pq; 14.60.St; 26.35.+c; 95.30.-k

I. INTRODUCTION

The role of neutrinos in primordial nucleosynthesis has been exploited to infer constraints on the number of leptons and light neutrinos in the Standard Model of particle physics [1]. Complimentary to this, the width of the Z_0 was found to allow only three light weakly-coupled neutrinos [2]. This experimental determination of the number of neutrinos, N_ν, has led some to describe primordial nucleosynthesis as determined by only one parameter: the baryon-to-photon ratio, η. Along with the assumptions of homogeneity and isotropy, the theory of Standard Big Bang Nucleosynthesis (SBBN) predicts the abundance of the lightest nuclides within reasonable error through the single parameter η.

Now, however, indications of neutrino oscillations from the atmospheric muon neutrino deficit, the solar neutrino deficit and the LSND excess may prove that our understanding of neutrino physics is incomplete [3]. This uncertainty in neutrino physics threatens to destroy the aesthetics of a one parameter SBBN with the several parameters of the neutrino mass and mixing matrix.

Neutrino mixing in the early universe can induce effects including matter-enhanced neutrino flavor transformation, partial thermalization of extra degrees of freedom, and lepton number generation. Efforts are sometimes made to crowd the multiple effects of neutrino mixing into a single parameter, $N_\nu^{\rm eff}$, the effective number of neutrinos.

The kinetic equations describing the effects of neutrino mixing in the early universe were first discussed by Dolgov [4]. Larger δm^2 and $\sin^2 2\theta$ accelerate population of sterile states. Resonant conversion of active neutrinos to sterile neutrinos may also take place when the mass eigenvalue corresponding to ν_s is smaller than that for the ν_α, *i.e.*, $m_s^2 - m_\alpha^2 = \delta m_{s\alpha}^2 < 0$. Both resonant and non-resonant conversion has been used to place constraints on active-sterile neutrino properties [5–7].

Several formulations of neutrino dynamics in the early universe evolve the system at a monochromatic average neutrino energy with interactions occuring at an integrated rate. This approach is appropriate when the time scale of interactions between the neutrinos and

the thermal environment is much shorter than the dynamic time scale of neutrino flavor transformations. However, when tranformations and the Hubble expansion are more rapid than thermalization, neutrino energy distributions can be distorted from a Fermi-Dirac form. Furthermore, such spectral distortions can survive until nucleosynthesis [8]. The role of neutrino energy distributions in primordial nucleosynthesis has been discussed since the earliest work on the subject [9,10]. Recent work [11,12] has emphasized the importance of neutrino energy distributions on the weak nucleon interconversion rates ($n \rightleftharpoons p$). Kirilova and Chizhov [11] included the distortion of neutrino spectra from nonresonant transformations in their nucleosynthesis calculation. A time-evolving distortion was also included in a calculation of helium production after a neutrino-mixing-generated lepton asymmetry in electron-type neutrinos from $\nu_e \rightleftharpoons \nu_s$ or $\bar{\nu}_e \rightleftharpoons \bar{\nu}_s$ (active-sterile) mixing [12].

In this paper we explore in detail the effects on primordial nucleosynthesis of the non-thermal neutrino spectra produced by the resonant transformations discussed in [12]. The resonant transformation of electron-type neutrinos to steriles can leave a near absence of neutrinos in the low energy end of the active neutrino energy spectrum. We find that this suppression of low energy neutrinos or anti-neutrinos in the otherwise Fermi-Dirac spectrum alters the neutron-to-proton weak interconversion reactions. These alterations stem from initial and final phase space effects.

Specifically, we find that the absence of low energy electron anti-neutrinos lifts the Fermi blocking of final state neutrinos in neutron decay. In addition, the absence of low energy electron neutrinos capturing on neutrons significantly alters the rate of this interaction. Both cases lead to an alteration of the neutron-to-proton ratio at weak freeze out, which is directly related to the produced mass fraction of primordial helium.

II. THE DYNAMICS OF NEUTRINO TRANSFORMATION

The general equations describing the evolution of M flavors of neutrinos in a high density environment such as the early universe are derived from the evolution equation for the density

operator

$$i\frac{\partial\rho}{\partial t} = [H, \rho]. \tag{1}$$

Here ρ can be the density operator for the entire system of M neutrinos or any smaller neutrino system that evolves rather independently of the other neutrino mixings. Several authors [4,5,11] explicitly follow the evolution of neutrinos through the density matrix.

The evolution of the density operator for a two state active-sterile system has been popularized in a vector formalism where the density operator is

$$\rho = \frac{1}{2}P_0(1 + \mathbf{P}\cdot\sigma) \qquad \bar{\rho} = \frac{1}{2}\bar{P}_0(1 + \bar{\mathbf{P}}\cdot\sigma) \tag{2}$$

where $\bar{\rho}$, $\bar{\mathbf{P}}$ and $\bar{P}_0$ refer to the anti-neutrino states. For an active-sterile two state system, the Hamiltonian of eqn. (1) includes forward scattering off of the $e^{\pm}$ background, and elastic and inelastic scattering of neutrinos from all leptons (see, *e.g.*, Ref. [13]). For this system, substituting (2) into the evolution equation resulting from Eqn. 1 gives

$$\frac{d}{dt}\mathbf{P} = \langle\mathbf{V}\rangle \times \mathbf{P} + (1 - P_z)\left(\frac{d}{dt}\ln P_0\right)\hat{\mathbf{z}} - \left(D^E + D^I + \frac{d}{dt}\ln P_0\right)(P_x\hat{\mathbf{x}} + P_y\hat{\mathbf{y}}) \tag{3}$$

$$\frac{d}{dt}P_0 = \sum_{\alpha=e,\nu_\mu,\nu_\tau} \langle\Gamma(\nu_e\bar{\nu}_e \to \alpha\bar{\alpha})\rangle(\lambda_\alpha n_\alpha n_{\bar{\alpha}} - n_{\nu_e} n_{\bar{\nu}_e}) \tag{4}$$

where an average over the momentum ensemble of neutrinos is taken for the vector potential $\mathbf{V}$ and the interaction rates Γ. Here D^I and D^E are the damping coefficients due to inelastic and elastic neutrino scattering off of $e^{\pm}$ and themselves (see [7]). Also, $\lambda_\nu = \frac{1}{4}$ and $\lambda_e = 1$. This set of equations (3,4) can be followed for specific neutrino momenta. An initial thermal neutrino spectrum can be discretized into $\mathcal{N}$ energy bins. Along with the number density evolution equations of neutrinos that do not undergo transformation, these equations form $8\mathcal{N}$ equations describing the evolution of the system.

Here we assume that the sterile neutrino sea is unpopulated at a temperature $T \sim 100\,\mathrm{MeV}$ (see Ref. [14]). Active neutrinos can undergo resonant transformation to sterile neutrinos as the density of $e^{\pm}$ decreases with the expansion. As in the sun, the resonance point is energy dependent. For example, the resonance, for $\delta m^2_{s\alpha} < 0$, occurs at

$$\left(\frac{E}{T}\right)_{\rm res} \approx \frac{|\delta m^2/{\rm eV}^2|}{16(T/{\rm Mev})^4 L_{\nu_\alpha}}, \tag{5}$$

where E/T is the neutrino energy scaled by the ambient temperature. This resonance adiabatically converts $\nu_\alpha(\bar{\nu}_\alpha)$ to $\nu_s(\bar{\nu}_s)$ as long as the timescale of the resonance is much longer than the neutrino oscillation period at resonance, and the resonance position must move slowly through the neutrino energy spectrum (see Ref. [12]).

As the universe expands and the ambient temperature decreases, the resonance moves from lower to higher neutrino energies. The energy-dependence of the resonance becomes important at temperatures below $T_{\rm dec} \approx 3\,{\rm MeV}$ [8]. Below this temperature, the neutrinos decouple from the $e^\pm$ background. The weak interaction rates of elastic and inelastic scattering of neutrinos above $T_{\rm dec}$ are much faster than the expansion time scale. In this case, the neutrino energy distributions can reshuffle into a thermal Fermi-Dirac spectrum before the onset of nucleosynthesis. However, if the transformation occurs after decoupling, the expansion rate will be too rapid, and therefore the neutrino spectra enter the epoch of nucleosynthesis in a non-thermal state. This will be the case, usually, when the mass-squared difference between mass eigenvalues corresponding to ν_e and ν_s is $|\delta m^2_{es}| \leq 1\,{\rm eV}^2$.

Direct $\nu_e \rightarrow \nu_s(\bar{\nu}_e \rightarrow \bar{\nu}_s)$ transformation was explored by Foot and Volkas [15] as a possible means to allow for a sterile neutrino within SBBN with minimal modification to the theory, and also to reduce the difference between the ^{4}He abundance predicted by the observed primordial deuterium abundance [17] and the primordial ^{4}He abundance inferred by Olive *et al.* [16]. The change in primordial helium production in this $\nu_e \rightarrow \nu_s(\bar{\nu}_e \rightarrow \bar{\nu}_s)$ scenario, including alterations of neutrino spectra, was described in [12]. The resonant transformation of $\nu_e \rightarrow \nu_s(\bar{\nu}_e \rightarrow \bar{\nu}_s)$ produces a lepton number asymmetry in electron-type neutrinos, L_{ν_e}. Here we define the net lepton number residing in neutrino species ν_α to be $L_{\nu_\alpha} \equiv (n_{\nu_\alpha} - n_{\bar{\nu}_\alpha})/n_\gamma$, where n_{ν_α}, $n_{\bar{\nu}_\alpha}$, and $n_\gamma = (2\zeta(3)/\pi^2)T^3$ are the proper number densities of ν_α, $\bar{\nu}_\alpha$, and photons, respectively. The sign of this asymmetry depends sensitively on initial thermal conditions and can be different in causally disconnected regions [18,19]. In the following sections, we address how non-thermal spectra affect the production

of primordial helium.

III. WEAK NUCLEON INTERCONVERSION RATES AND PRIMORDIAL HELIUM

Since nearly all of the neutrons present during primordial nucleosynthesis go into ^{4}He nuclei, the production of primordial helium in the early universe is dominated by the abundance of neutrons relative to protons. The weak nucleon interconversion reactions

$$n + \nu_e \rightleftharpoons p + e^- \qquad n + e^+ \rightleftharpoons p + \bar{\nu}_e \qquad n \rightleftharpoons p + e^- + \bar{\nu}_e.$$

are in steady state equilibrium at temperatures $T > 0.7\,\mathrm{MeV}$. The neutron-to-proton ratio (n/p) freezes out of equilibrium when the weak nucleon interconversion rates fall below the expansion rate (see Fig. 1). The "frozen" n/p ratio slowly evolves as free neutrons decay until the epoch ($T \sim 0.1$ MeV) when almost all neutrons are incorporated into alpha particles ("nucleosynthesis"). In steady state equilibrium, n/p can be approximated by the ratio of the nucleon interconversion rates,

$$\frac{n}{p} \approx \frac{\lambda_{p\to n}}{\lambda_{n\to p}}.$$

The evolution of n/p is followed numerically in detail in Kawano's [20] update of Wagoner's code [10]. The suppression of low energy electron-type neutrinos affects the rates of the six weak nucleon reactions differently.

If sterile neutrinos are partially or completely thermalized, they will increase the expansion rate since they will contribute to the energy density of the primordial plasma. The expansion rate, H, is related to the total energy density, $\rho_{\rm tot}$ and the cosmological constant, Λ as [10,20]

$$H = \sqrt{\frac{8\pi}{3} G \left(\rho_{\rm tot} + \frac{\Lambda}{3}\right)}.$$

In general, an increase to the energy density and expansion rate will increase n/p at freeze-out, and thus increase the primordial ^{4}He yield, Y_p. The contribution to the expansion rate

is not significant for $\nu_e \to \nu_s(\bar{\nu}_e \to \bar{\nu}_s)$ conversion post-decoupling, since the energy density in electron-type neutrinos is just transferred to steriles without further thermal creation of neutrinos (since they have decoupled from the $e^{\pm}$ plasma before the onset of transformation).

For the case where $L_{\nu_e} < 0$, the reactions influenced by the ν_e distortion are the forward and reverse reactions of $n + \nu_e \rightleftharpoons p + e^-$. Because of the neutron/proton mass difference, very low energy neutrinos readily participate in $n + \nu_e \to p + e^-$. Here, the neutrino energy is $E_\nu = E_e - Q > 0$, where $Q \equiv m_n - m_p$ is the nucleon mass difference, and E_e is the electron energy. The suppression of low energy neutrinos impacts this reaction by significantly limiting the phase space of initial states of the interaction. The neutrino energy distribution is accounted for in the $n + \nu_e \to p + e^-$ rate integral in the following manner:

$$\lambda_{n\nu\to pe} = A \int v_e E_e^2 p_\nu^2 dp_\nu [e^{E_\nu/kT_\nu} + 1]^{-1} [1 + e^{-E_e/kT}]^{-1}. \tag{6}$$

The rate of the reaction $p + e^- \to n + \nu_e$ is given by

$$\lambda_{pe\to n\nu} = A \int E_\nu^2 p_e^2 dp_e [e^{E_e/kT} + 1]^{-1} [1 + e^{-E_\nu/kT_\nu}]^{-1}. \tag{7}$$

In these equations we have used Weinberg's notation [21]. The deficit in low energy neutrinos renders the integrand of (6) to be nearly zero for energy ranges where ν_e have transformed to steriles (see Fig. 2). The reaction $p + e^- \to n + \nu_e$ is altered by a lifting of Fermi-blocking $[1 + e^{-E_\nu/kT_\nu}]^{-1}$ at low energies because of the reduction of low energy neutrino numbers. However, the rate $\lambda_{pe\to n\nu}$ is changed less significantly than $\lambda_{n\nu\to pe}$ and thus affects n/p less. This can be seen in Fig. 4 (a), where the change in rate with respect to the overall $n \to p(p \to n)$ rate is shown for rate (2) $\lambda_{n\nu\to pe}$ and (6) $\lambda_{pe\to n\nu}$.

For $L_{\nu_e} > 0$, the reactions affected by $\bar{\nu}_e$ distortion are $n + e^+ \rightleftharpoons p + \bar{\nu}_e$ and $n \rightleftharpoons p + e^- + \bar{\nu}_e$. In the forward and reverse reactions $n + e^+ \rightleftharpoons p + \bar{\nu}_e$, the escaping or incident $\bar{\nu}_e$ must have an energy $E_{\bar{\nu}_e} = Q + E_e \geq 1.804\,\mathrm{MeV}$. Even for the case we examined with the greatest spectral distortion ($|\delta m_{se}^2| = 1\,\mathrm{eV}^2$), the spectral cutoff never extends above $E_{\bar{\nu}_e} = 1.35\,\mathrm{MeV}$. Therefore, $n + e^+ \rightleftharpoons p + \bar{\nu}_e$ is not altered by this low energy distortion (see Fig. 4 (b)). The interaction $p + e^- + \bar{\nu}_e \to n$ makes a very small contribution to $\lambda_{p\to n}$, and modifications of

its rate are not important to n/p at freeze-out. The only significant reaction rate affected by the $\bar{\nu}_e$ distortion is neutron decay: $n \rightarrow p + e^- + \bar{\nu}_e$ (Fig. 4). The reaction is limited in SBBN by Fermi-blocking of low-energy $\bar{\nu}_e$ products. This blocking is lifted when low-energy $\bar{\nu}_e$ transform to ν_s. The integrand of the neutron decay rate

$$\lambda_{n\rightarrow pe\nu} = A \int v_e E_\nu^2 E_e^2 dp_\nu [1 + e^{-E_\nu/kT_\nu}]^{-1} [1 + e^{-E_e/kT_\nu}]^{-1} \tag{8}$$

can be seen in Fig. 3 for the most dramatic case of $|\delta m^2| = 1\,\mathrm{eV}^2$. The Fermi-blocking term, $[1 + e^{-E_\nu/kT_\nu}]^{-1}$, is unity for low energy neutrinos that have transformed to steriles.

The change in $\lambda_{n\nu\rightarrow pe}$ (for $L_{\nu_e} < 0$) is significantly larger than that for $\lambda_{n\rightarrow pe\nu}$ (for $L_{\nu_e} > 0$). The change in helium mass fraction (Y_p) produced by BBN for $L_{\nu_e} < 0$ is $\delta Y_p \simeq 0.022$, while a $L_{\nu_e} > 0$ correspondingly causes smaller a change of $\delta Y_p \simeq -0.0021$ [12].

In summary, if electron-type neutrino spectra are altered through matter-enhanced transformation and survive until nucleosynthesis, they can modify $n \rightleftharpoons p$ interconversion rates through the availability of initial and final neutrino energy states. This kind of scenario is realized in $\nu_e \rightarrow \nu_s(\bar{\nu}_e \rightarrow \bar{\nu}_s)$ matter-enhanced transformations with $|\delta m^2| \leq 1\,\mathrm{eV}^2$. Non-thermal $\nu_e/\bar{\nu}_e$ spectra will arise in any case where flavor transformations occur near or below $T_{\rm dec}$ between a more-populated electron-type neutrino and some other less-populated neutrino flavor, and will produce the same kinds of limitations on reaction phase space as the resonance point goes from lower to higher neutrino energies. The effects of non-thermal electron-type neutrino distributions will then need to be included.

ACKNOWLEDGMENTS

K. A., X. S., and G. M. F. are partially supported by NSF grant PHY98-00980 at UCSD. K. A. acknowledges partial support from the NASA GSRP program.

---

[1] G. Steigman, D. N. Schramm & J. R. Gunn, *Phys. Lett.* **B 66**, 202 (1977).

[2] Particle Data Group, *Review of Particle Physics*, *European Physical Journal* **C3**, 1 (1998).

[3] D. O. Caldwell, *Int. J. Mod. Phys.* **A13**, 4409 (1998); J. M. Conrad, Plenary Talk presented at the International Conference on High Energy Physics (ICHEP), Vancouver, 1998, hep-ex/9811009.

[4] A. D. Dolgov, *Sov. J. Nucl. Phys.* **33**, 5.

[5] R. Barbieri and A. Dolgov, *Phys. Lett.* **B 237**, 440 (1990); *ibid.*, *Nucl. Phys.* **B 349**, 743 (1991).

[6] K. Enqvist, K. Kainulainen and M. Thomson, *Nuc. Phys.* **B 373**, 498 (1992).

[7] X. Shi, D. N. Schramm and B. D. Fields, *Phys. Rev.* **D48**, 2563 (1993).

[8] M. J. Savage, R. A. Malaney & G. M. Fuller, *Astrophys. J.***368**, 1 (1991).

[9] R. A. Alpher, J. W. Follin, Jr. and R. C. Herman, *Phys. Rev* **92**, 1347 (1953).

[10] R.V. Wagoner, W.A. Fowler and F. Hoyle, *Astrophys. J.* **148** 3 (1967).

[11] D. P. Kirilova & M. V. Chizhov, *Phys. Rev.* **D58**, 073004 (1998).

[12] X. Shi, G. M. Fuller and K. Abazajian, *Phys. Rev.* **D 60**, 063002 (1999).

[13] B. McKellar, and M. J. Thomson, *Phys. Rev.* **D 49**, 2710 (1994).

[14] G. M. Fuller & R. A. Malaney. *Phys. Rev.* **D 43**, 3136 (1991).

[15] R. Foot and R. R. Volkas, *Phys. Rev.* **D 56**, 6653 (1997).

[16] K. Olive, G. Steigman and E. Skillman, *Astrophys. J.* **483**, 788 (1997).

[17] S. Burles and D. Tytler, *Astrophys. J.***499**, 699 (1998); *ibid.*, *Astrophys. J.***507**, 732 (1998); D. Tytler, X. Fan and S. Burles, *Nature* **381**, 207 (1996).

[18] X. Shi, *Phys. Rev.* **D 54**, 2753 (1996).

[19] X. Shi and G. M. Fuller astro-ph/9904041 (unpublished).

[20] L. Kawano, FERMILAB-PUB-92-04-A, Jan 1992.

[21] S. Weinberg, *Gravitation and Cosmology*, J. Wiley, New York (1972).

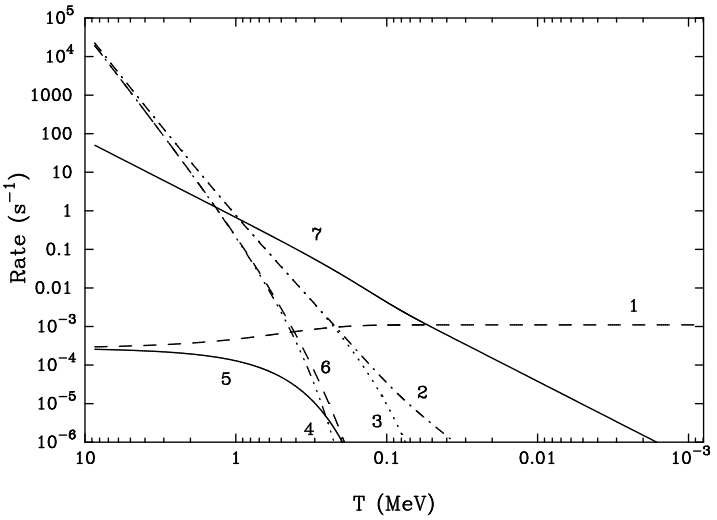

FIG. 1. The evolution of the $n \rightleftharpoons p$ rates are shown. 1) $n \rightarrow p + e^- + \bar{\nu}_e$, 2) $n + \nu_e \rightarrow p + e^-$, 3) $n + e^+ \rightarrow p + \bar{\nu}_e$ 4) $p + \bar{\nu}_e \rightarrow n + e^+$, 5) $p + e^- + \bar{\nu}_e \rightarrow n$, 6) $p + e^- \rightarrow n + \nu_e$ 7) The Hubble expansion rate, when the rates fall below the expansion rate, n/p "freezes" out.

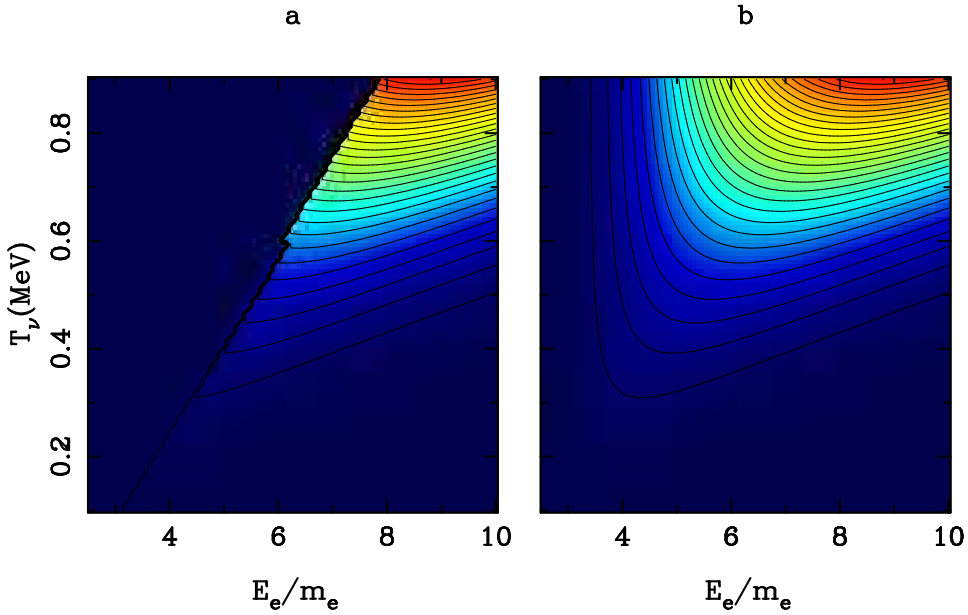

FIG. 2. Plotted are the contours of the amplitude of the rate integrand for $n + \nu_e \rightarrow p + e^-$, with increasing amplitude towards the upper right: (a) shows the blocking of the integrand for lower energies due to the suppression of low energy electron neutrinos; (b) shows the standard BBN integrand.

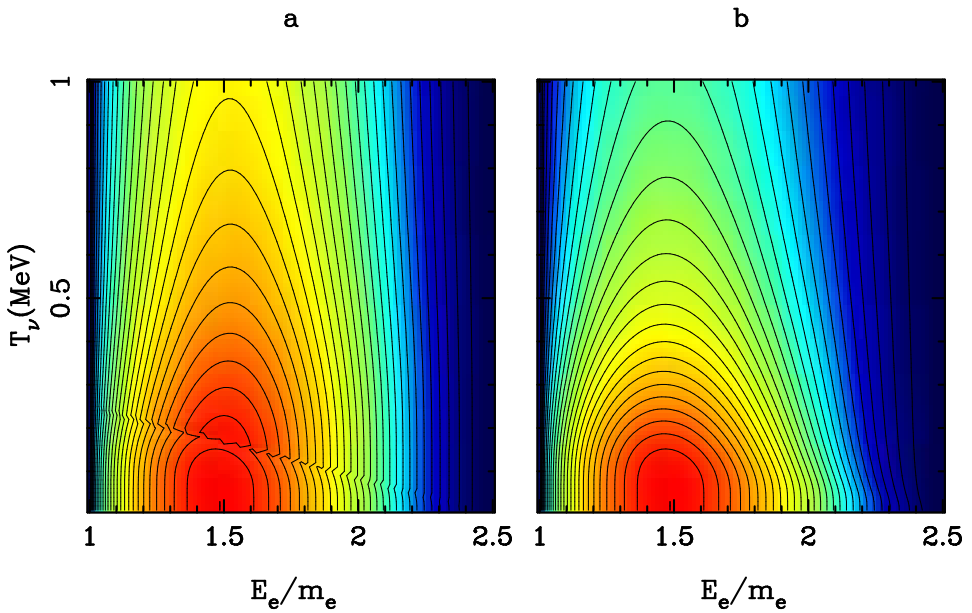

FIG. 3. Plotted are the contours of the amplitude of the rate integrand for $n \rightarrow p + e^- + \bar{\nu}_e$, with increasing amplitude towards the center. (a) shows the lack of Fermi blocking by low energy $\bar{\nu}_e$ at higher temperatures. (b) shows the standard BBN integrand.

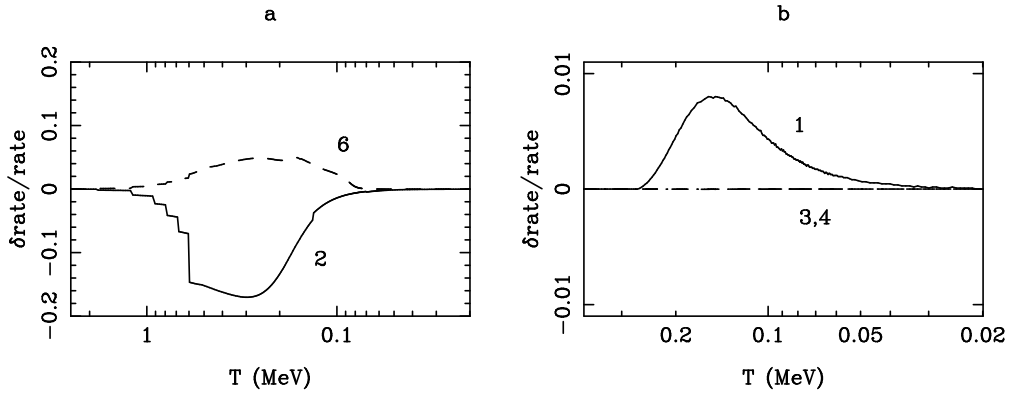

FIG. 4. Plotted are a) the change in rate 2. $n + \nu_e \rightarrow p + e^-$, 6. $p + e^- \rightarrow n + \nu_e$; and b) 1. $n \rightarrow p + e^- + \bar{\nu}_e$, 3. $n + e^+ \rightarrow p + \bar{\nu}_e$ 4. $p + \bar{\nu}_e \rightarrow n + e^+$